Computer Model of Ethosuximide's Effect on a Thalamic Neuron

William W. Lytton, MD,* and Terrence J. Sejnowski, PhD*†

Ethosuximide appears to have a specific effect on the low-threshold calcium current in thalamic cells. This may be related to its efficacy in the treatment of absence epilepsy. We used a computer model of an individual thalamocortical neuron to better understand the alteration in the low-threshold calcium current under voltage clamp and to predict response to current injection in the presence of ethosuximide. The full model included nine voltage-sensitive ionic channels and a realistic dendritic morphology. The model reproduced the two major responses seen in tissue slices: repetitive spiking with depolarization and the low-threshold calcium spike elicited on release from hyperpolarization. The alteration in low-threshold calcium current with ethosuximide can be explained by a 10-mV depolarizing shift in the steady-state activation curve for this channel with a 10% reduction in maximum channel permeability. Simulations of current injection showed that ethosuximide diminished the low-threshold calcium spike while leaving the tonic firing pattern unaffected. Our results support the hypothesis that ethosuximide's effects on low-threshold calcium current might selectively alter the dynamics of slow bursting in thalamic cells.

Lytton WW, Sejnowski TJ. Computer model of ethosuximide's effect on a thalamic neuron. Ann Neurol 1992;32:131–139

Recent studies have shown that ethosuximide, an anticonvulsant that selectively prevents absence (petit mal) epilepsy [1, 2], affects the low-threshold calcium current (LTCC) [3, 4]. This current is mediated by a voltage-sensitive calcium channel present at a high density in thalamic neurons. The effect of ethosuximide on the LTCC is not matched by other anticonvulsants with different therapeutic uses or by similar compounds without antiabsence effects [3, 5]. The thalamus plays a role in the characteristic, three-per-second spike-and-wave rhythm of absence epilepsy seen both in patients and in animal models [6, 7] and ethosuximide has been found to block the genesis of similar rhythms elicited by electrical stimulation in vivo [8]. The LTCC is essential for the generation of the low-threshold calcium spike (LTCS) which underlies slow thalamic rhythms [9, 10]. Therefore, it has been suggested that ethosuximide's therapeutic action may be due to this interference with the LTCS [3].

In vitro intracellular current- and voltage-clamp recording can be of use in understanding the relationship between pharmacological agents and therapeutic efficacy in physiological disorders such as epilepsy. In voltage clamp, the membrane potential is held constant by varying the injected current to compensate for currents passing through voltage-sensitive ion channels. Voltage clamp is used to study the kinetics of individual voltage- or ligand-sensitive ion channels that underlie both synaptic and intrinsic membrane potentials. Voltage-clamp data provide a detailed view of one type of channel, isolated by blocking others. In contrast, the behavior of the neuron as a whole can be studied with current clamp, during which injected current is held constant. The membrane potential is allowed to change, permitting exploration of the dynamics of neuron spiking under conditions that are closer to its native state. Voltage clamp and current clamp have complementary roles: Voltage clamp fills in the detailed kinetics of the many individual channels of the neuron and current clamp shows how these currents interact to produce neuronal firing.

Studies of absence epilepsy have progressively focused in on the details of the underlying mechanisms. After initial patient studies implicated the thalamus in absence epilepsy, in vivo animal studies added to our understanding of corticothalamic interaction. Subsequently, current clamp was used to observe the behavior of single thalamic cells and voltage clamp was used to uncover ion channel kinetics. Computer modeling can help in fitting these microscopic observations into the broader scope of physiology. Models organize knowledge across many different levels of investigation and make it possible to understand the implication of ion channel kinetics for the firing of the cell, for inter-

From *The Salk Institute and †Howard Hughes Medical Institute, La Jolla, CA.

Received Sep 18, 1991, and in revised form Jan 27, 1992. Accepted for publication Jan 28, 1992.

Address correspondence to Dr Lytton, The Salk Institute, 10010 N. Torrey Pines Road, La Jolla, CA 92037.

actions of thalamic neurons with cortex, and ultimately, for the patient's disease and its treatment. In the present study, we take the first step by modeling voltage-clamp data and using the results to predict the effect of ethosuximide on current-clamp recording of thalamic cells.

Materials and Methods

Simulations were performed using a modified version of Hines' CABLE simulator on a MIPS Magnum 3000 computer (MIPS Computer Systems, Inc. Sunnyvale, CA) [11]. Simulations were run with a time step of 25 μsec. Shorter time steps were used to test the accuracy of the numerical integration.

In the simulations presented, voltage-sensitive channels were present only in the soma, due to the difficulty in obtaining data for channel densities in dendritic locations. Such information will eventually have to be obtained and incorporated in future models. We did, however, assess the effect of placing the calcium channels 50 μm out in the dendrites. Although space clamp was incomplete at this distance, the shift in the activation curve was relatively minor. Therefore, a two-compartment model was used for subsequent voltage-clamp simulations.

A realistic thalamic cell morphology was used for all current-clamp simulations in order to obtain realistic impedance characteristics. The morphology was obtained by C-F. Hsiao and M. Dubin (University of Colorado, Denver, CO) using a Eutectics neuron-tracing system and provided to us by J. Capowski of Eutectics (Eutectics Electronics, Raleigh, NC). The morphology of this lateral geniculate nucleus (LGN) neuron is similar to that of other principal thalamic neurons (Fig 1) [12]. The cell was represented in the model by either 57 or 134 compartments. Similar results were obtained with both discretizations. Soma area was 1,275 μm^2. Membrane capacitance was assumed to be 1 $\mu F/cm^2$ and longitudinal residence was 175 $\Omega \cdot cm$.

For the current-clamp studies, nine channels were included as described by Steriade and Llinás [13]. In addition to a modified Hodgkin-Huxley fast sodium (I_{Na}) and delayed rectifier (I_{Kd}) currents [14, 15], the model included persistent sodium current (I_{NaP}); an LTCC and a noninactivating high-threshold calcium current (HTCC); the potassium currents I_A, I_M, and I_C; and the mixed current I_H, which is carried by both sodium and potassium ions. Calcium was removed from the model cell by radial diffusion, a sodium-calcium exchange mechanism, and a calcium ATPase pump. Except for I_H and LTCC, whose parameters are described below, the equations describing the channels and pumps were identical to those used in a previous study [16]. Although channel kinetics were taken from many sources, it was possible to obtain firing patterns characteristic of thalamic cells by adjusting the channel density represented by maximal permeability ($\bar{p}$, in cm/sec) for calcium channels and maximal conductance ($\bar{g}$, in siemens/cm^2) for all other channels. Calcium currents were calculated using the Goldman-Hodgkin-Katz equation to allow for the nonlinearity caused by the large calcium concentration gradient [17].

Characteristic values for channel density parameters were as follows: $\bar{g}_{Na}$ of 1.0, $\bar{g}_{NaP}$ of $5 \cdot 10^{-5}$, $\bar{g}_{Kd}$ of 0.05, $\bar{g}_A$ of

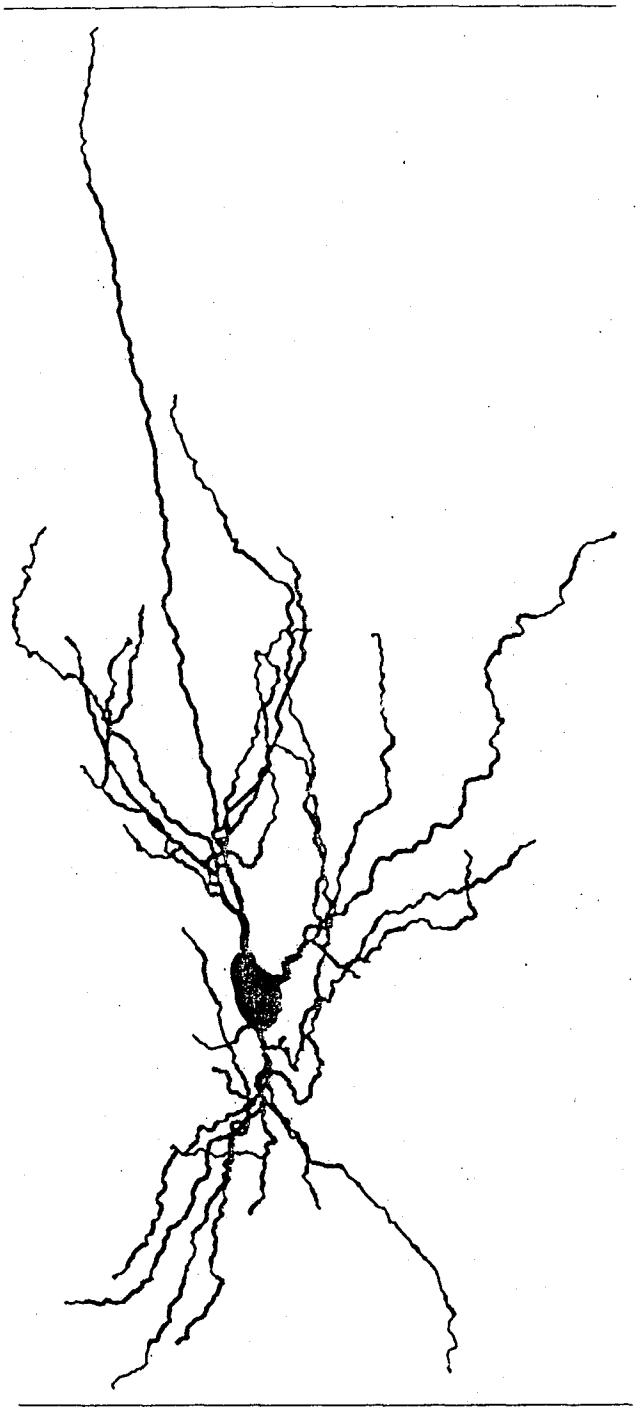

Fig 1. Morphology of a thalamic cell used in the compartment model. This tracing of a lateral geniculate nucleus neuron was prepared for light microscopy using the Golgi method and traced with a Eutectics neuron-tracing system by Drs Hsiao and Dubin. The cell was represented in the model by 134 separate compartments representing different parts of the dendritic tree and the soma. Spines were not represented in the model. Active channels were confined to the soma. (Courtesy of Drs Chie-Fang Hsiao and Mark Dubin, University of Colorado.)

0.02, $\bar{g}_M$ of $4 \cdot 10^{-4}$, $\bar{g}_C$ of 0.04, and $\bar{g}_H$ of 0.0018 siemens/cm^2, and $\bar{p}_{LTCC}$ of $6 \cdot 10^{-4}$, and $\bar{p}_{HTCC}$ of $8 \cdot 10^{-5}$ cm/sec. The leakage conductance was $6 \cdot 10^{-5}$ siemens/cm^2 except in the soma where it was adjusted to provide a resting membrane potential (RMP) of -65 mV. Soma leakage conductance depended on the resting conductances of active channels present for a particular set of parameters and was typically about $7 \cdot 10^{-4}$ siemens/cm^2. The input impedance of the cell was 65 MΩ with a membrane time constant of 9 msec. The low apparent input impedance was due primarily to the action of the anomalous rectifier, I_H [17]. In its absence, input impedance was 113 MΩ with a 16-msec membrane time constant. These values are within the range observed in LGN in cat and rat [18, 19].

The LTCC was modeled using data from several sources [20–22]. As in the original voltage-clamp study on ethosuximide's effect [3], both m_∞ and h_∞ were described by the Boltzmann equation of the form

$$x_\infty = 1/\left(1 + e^{(V - V_{1/2})/K}\right), \quad (1)$$

where $V_{1/2}$ is voltage of half-maximal activation or inactivation and K is a parameter setting the slope of the curve, negative for m_∞ and positive for h_∞. As in the previous study [20], the activation variable m entered as third order in calculating the final permeability:

$$P_{LTCC} = \bar{P}_{LTCC} \cdot m^3 \cdot h \quad (2)$$

As a result, the steady-state activation is m_∞^3. In what follows, we will give parameters detailing shifts in the m_∞ curve. The shift of the m_∞^3 curve is comparable. The voltage-dependent time constants for LTCC were taken directly from the original studies using interpolation and were not parameterized by curve fitting. We were therefore able to alter the activation curve without a corresponding shift in channel time constants. Although this is not possible when all of the transition rates are equal, as in the Hodgkin-Huxley model, in other channel models the relationship between time constant and activation functions can be more complex [17, 23].

I_H was modeled from the data of McCormick and Pape [24] obtained from a thalamic cell. Because this channel shows activation only, with no inactivation, they obtained time constants for both activation and deactivation instead of the single time constant of activation described in most studies. We interpreted these time constants, taken from fully deactivated and fully activated states, respectively, as being the inverse of the kinetic rates describing a two-state channel model. Using the Hodgkin-Huxley parameterization of the two-state model, we calculated our time constant as the inverse of the sum of these voltage-dependent rates ($\tau = 1/[\alpha + \beta]$). We used the experimentally obtained I/I_{max} as the steady-state activation for our simulations.

Voltage-clamp data were obtained from the literature by scanning figures on an Apple scanner (Apple Computer, Inc, Cupertino, CA). The digitized image was then edited to remove everything but the data points using the image-processing program Image (Wayne Rasband, National Institutes of Health Research Services Branch, National Institute of Mental Health). *Image* was then used to locate each data point in x-y pixel coordinates. The values were normalized to obtain scaled values.

Results

The phenomena described in this article were seen in our initial, relatively simple models and persisted across many variations in types of channels used, channel density, form of activation equations, and cell morphology. In all, approximately 1,500 simulations were performed. The models invariably showed that the alteration of the LTCC in response to voltage clamp in the presence of ethosuximide is consistent with an alteration of response to current clamp, as had been previously postulated. Ethosuximide's effect on the LTCC can be expected to curtail or eliminate low-threshold spikes while leaving other responses intact.

Model of Low- and High-Threshold Calcium Currents from Voltage-Clamp Data

We used data from three different voltage-clamp studies of the LTCC in the thalamus [20–22], as well as an earlier study in sensory neurons [25], as starting points for directly modeling the voltage-clamp traces in the ethosuximide study [3]. These thalamic studies differed in the species of animal, in the area of thalamus assessed, and in recording technique, but obtained largely comparable results. Our voltage-clamp model also included the non-inactivating HTCC. Parameters from a voltage-clamp study of HTCC in guinea pig hippocampus [26] gave an excellent match to the thalamic cell data. The relative permeabilities of the two currents were adjusted to provide both time course and maximal current amplitude comparable to those measured (Fig 2). This was produced with an LTCC permeability ($\bar{P}_{LTCC}$) of $7.7 \cdot 10^{-5}$ cm/sec and an HTCC permeability ($\bar{P}_{HTCC}$) of $7.3 \cdot 10^{-5}$ cm/sec. The LTCC parameters were $V_{1/2}$ of -55 mV and K of -12.0 mV for m_∞, and $V_{1/2}$ of -88 mV and K of 5.3 mV for h_∞. As we tried to model specific voltage-clamp traces taken from different cells, we modified both m_∞ and h_∞ for LTCC as well as LTCC and HTCC channel density. Many of these modifications were made as fine adjustments to more accurately fit the data. However, the density of the channels and the location of the m_∞ curve seemed to vary significantly from study to study. Variation in channel density is to be expected as a consequence of varying amounts of damage to cells in dissociation and may also reflect natural variation. Variation in m_∞ could also be due to variability in the precise voltage dependence of the LTCC channel population in different individual cells.

The original study of the LTCC showed that recovery from inactivation could not be completely described by a single exponential [4]. A recent model of the LTCC used two time constants to model this pro-

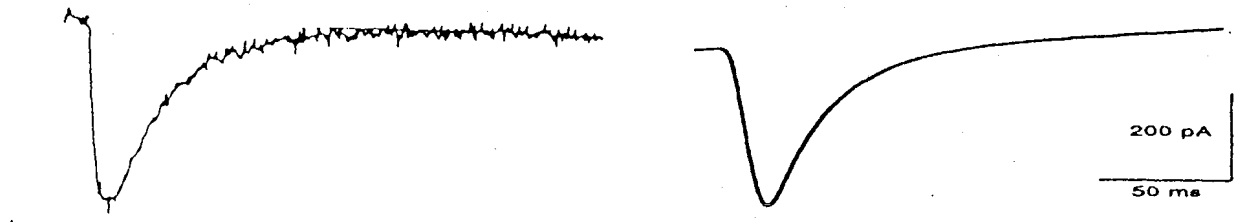
200 pA
50 ms

A

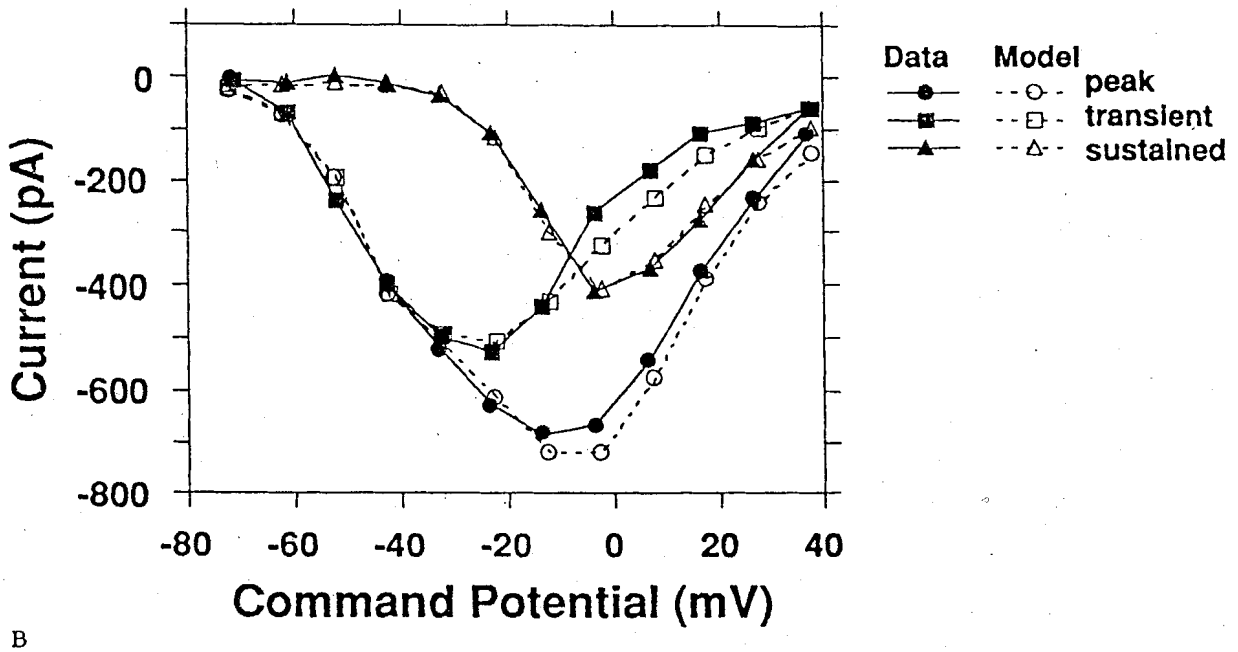
Data
Model
peak
transient
sustained
Current (pA)
0
-200
-400
-600
-800
-80
-60
-40
-20
0
20
40
Command Potential (mV)

B

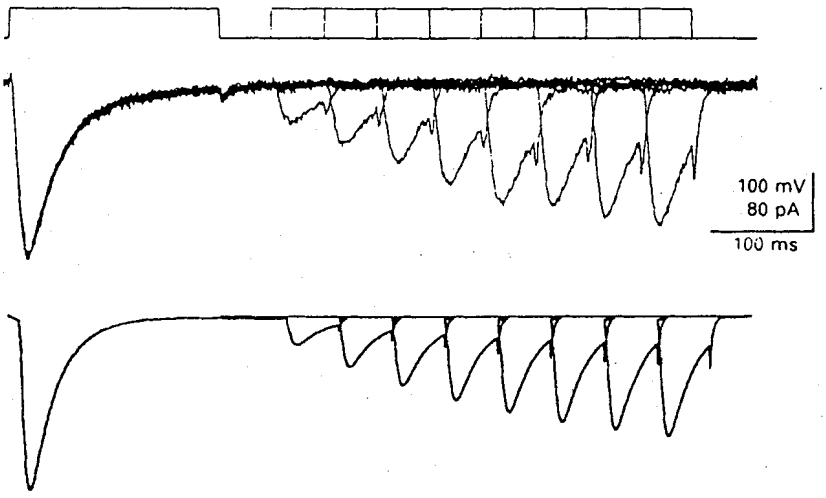
100 mV
80 pA
100 ms

C

cess [27]. We found that a single exponential model was adequate to reproduce the data given (Fig 2C). In any case, recovery from inactivation was not required in the initial response to current injection that we have modeled.

Model of Low-Threshold Calcium Current in Presence of Ethosuximide

Coulter and colleagues [4, 5] showed that the application of ethosuximide to isolated corticothalamic neurons reduced current flow through the LTCC but were not able to determine a single mechanism to explain the reduction. They explicitly assessed the voltage dependence of steady-state inactivation as well as the time course for activation, inactivation, and recovery from inactivation and concluded that none of these were altered. The reported shift in the onset of the calcium current to more depolarized potentials suggests that a shift in the LTCC steady-state activation curve in this direction might explain their findings. We replicated the control voltage-clamp response to different command voltages by using a $V_{1/2}$ of -58 mV and K of -7.8 mV for m_∞, and $V_{1/2}$ of -83.5 mV and K of 6.3 mV for h_∞ (Fig 3). The LTCC permeability in the control case was $4.6 \cdot 10^{-5}$ cm/sec with an HTCC permeability of $2.7 \cdot 10^{-5}$ cm/sec. A 10-mV depolarizing shift in m_∞ accompanied by a 10% reduction in channel density (to $4.2 \cdot 10^{-5}$ cm/sec) reproduced the shift in voltage-clamp response observed with ethosuximide (Fig 3B). The reduction in LTCC in the model is largely due to the elimination of the overlap between the activation and inactivation curves in the control condition (area under the intersection of m_∞ and h_∞ curves in Fig 3A).

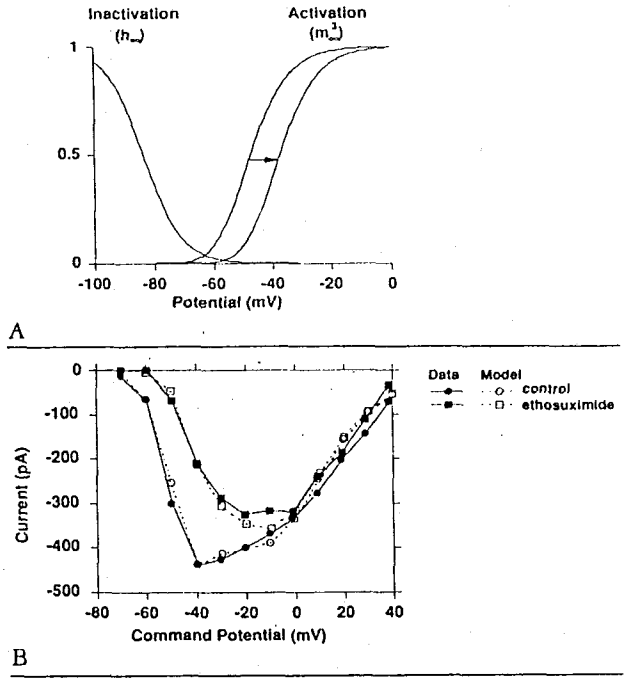

Fig 3. Comparison between the effects of ethosuximide on the model neuron and a principal thalamic neuron. (A) A 10-mV shift (arrow) *in steady-state activation reproduces the effect of ethosuximide. In this case, steady-state inactivation is given by m_∞^3 because the state variable m is cubed. The reduction in overall current is partly due to the reduction in the window of steady-state activation under the intersection of the two curves. (B) Peak current under voltage clamp to various command potentials from a holding potential of -100 mV. Activation in the control condition is compared to activation in the presence of ethosuximide. The approximate amount of the m_∞ shift can be estimated by noting that the current first activates at -70 mV in the control case and at -60 mV in the presence of ethosuximide. The two curves are approximately parallel at small depolarizations where there is little activation of the high-threshold calcium current. In this range, they approximate the slopes of the respective m_∞ curves. (Data from Coulter et al [3].)*

Fig 2. Calcium currents from voltage-clamp data compared to the model. (A) Voltage-clamp trace from a holding potential of -100 mV to a test potential of -40 mV shows activation of a transient calcium current with little persistent current. Experimental data (see Fig 1A, p 584 of [3]) are at left and model data, at right. (From Coulter et al [3] with permission.) (B) Peak current and sustained steady-state currents for voltage clamp from a holding potential of -100 mV to various command potentials, given on the abscissa. The approximate transient current is obtained by subtracting the sustained from the peak current. Since the high-threshold calcium current activates more rapidly than the low-threshold calcium current (LTCC), this difference closely approximates the LTCC. (Data from Coulter et al. [20].) (C) Recovery from inactivation of the LTCC. Voltage is initially stepped from -92 mV to -42 mV for sufficient time to cause full inactivation of the LTCC. On multiple runs, subsequent test pulses are given at different times to assess the degree of recovery from inactivation. Traces are shown superimposed. Experimental data are above (see Fig 7A, p 598 of [20]) and model data, below. (From Coulter et al [20] with permission.)

Manipulation of other model parameters did not reproduce the peak currents described (see Fig 3B). In particular, reduction of the LTCC maximum permeability decreased the amplitude at each point without altering the threshold voltage at which current flow started to appear. Manipulation of the HTCC only affected the amplitudes at higher voltages, as expected. Changing the activation time constant shifted the time of occurrence of the current peak but did not alter its amplitude.

Full Model Reproduces Responses to Current Injection

Jahnsen and Llinás [9, 28] described two distinct patterns of firing response to current injection in an in vitro thalamic slice preparation. They noted that an initial depolarization would produce a single spike or no spikes at all while further depolarization produced

repetitive firing at 50 to 100 Hz. Another characteristic firing pattern was a brief burst of one to four spikes following the cessation of hyperpolarizing current (the LTCS). This "anode break" effect was attributed to the presence of LTCCs in these cells. The hyperpolarization de-inactivates the channel since h, the Hodgkin-Huxley inactivation particle, increases at hyperpolarized voltages (see Fig 3A). Subsequent depolarization causes an increase in m towards m_∞. Since the time constant for m, τ_m, is shorter than that for h, τ_h, the product $m^3 \cdot h$ increases. This increased permeability (equation 2) produces an inward calcium flux giving the calcium spike.

We initially tried to obtain the LTCS using the density of calcium channels determined from the voltage-clamp study. Although with this density it was possible to produce an LTCS in the two-compartment model, there was not sufficient drive to produce an LTCS in the full model. The voltage-clamp studies were performed in acutely dissociated cells that had been enzymatically treated and shorn of their dendrites. These cells may have lost channels due to this procedure. Additionally, both voltage-clamp studies [20, 21] were conducted at room temperature (22°—24°C) while the current-clamp study [28] was performed at a physiological temperature (37°C). The LTCC shows a 3.3-fold increase in current amplitude with each 10°C increase in temperature (Q_{10} = 3.3) [20]. This value is consistent with a five-fold increase in permeability at a physiological temperature. With this change in the LTCC parameters, LTCSs could be elicited in the full model. The size of the LTCS was dependent on the exact form of m_∞ for the LTCC. Since this appears to be highly variable, we tried many different curves. In general, a larger, more robust LTCS could be obtained with a steeper m_∞ slope centered at more hyperpolarized voltages. The LTCS shown in Figure 4A was based on parameters obtained from Crunelli and associates [21]. We were able to reproduce both the LTCS and the tonic firing with several different sets of parameters both in the two-compartment model and in the full thalamic cell model.

Ethosuximide Abolishes the Low-Threshold Calcium Spike but Not Tonic Firing

Since the LTCS is dependent on the LTCC, we expected that the shift in activation would affect this firing pattern by requiring greater depolarization in order to reach the steep part of the activation curve where positive feedback gives a spike. Additionally, the shift in m_∞ significantly reduced the window created by the overlap of the activation and inactivation curves (see Fig 3A), reducing the voltage range where the channel conducts current without shutting off. Using the same hyperpolarizing current, the activation shift eliminated the LTCS for all parameter sets tested. Figure 4B shows the result using the same parameters as in Figure 4A but with the LTCC parameters altered to reflect the effect of ethosuximide. With most parameter sets, including that used in Figure 4B, it was still possible to obtain a reduced LTCS by injecting a much larger hyperpolarizing pulse. Despite this change, repetitive firing in response to depolarization was generally only slightly modified. In the example shown, the repetitive firing rate increased from 60 to 70 Hz. The increase in firing rate was due to the greater depolarization for a given current injection due to increased input impedance, a side effect of the reduction in leakage conductance needed to balance the reduced resting inward Ca^{2+}.

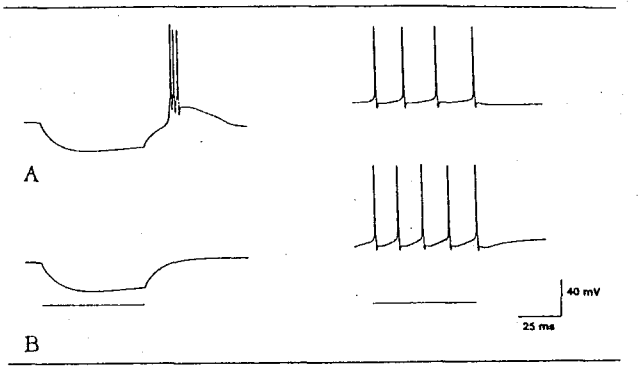

Fig 4. Model of low-threshold calcium spike (LTCS) and repetitive spiking under current clamp and effect of ethosuximide. (A) A hyperpolarizing pulse of 0.5 nA applied transiently is followed by LTCSs (left trace). *Tonic firing occurs when the model cell is presented with a 0.07-nA current injection following initial depolarization* (right trace). *Duration of injected current is indicated by lines at bottom. Traces are similar to those of Jahnsen and Llinás [9]. (B) Response in the model cell with the low-threshold calcium current altered to simulate the presence of ethosuximide. The same current steps are used. There is no longer any LTCS in response to a release from hyperpolarization* (left trace). *The tonic response to depolarization is still present but the rate of firing is increased from 60 to 70 Hz* (right trace).

Modification of Other Currents Can Also Affect the Low-Threshold Calcium Spike

The possibility that the LTCS might be a key to the initiation or maintenance of an absence seizure stimulated us to look for other manipulations of individual ion channels that might also affect it. Figure 5 shows time constants and voltage range for activation and inactivation of the channels involved in the thalamic cell model. The LTCC is active in the region of RMP, the range where the LTCS is initiated. The only other currents that are active in this range are the persistent sodium current (I_{NaP}) and the mixed inward current I_H. We did not consider the activity of the persistent sodium channel in any detail.

I_H is an inward current that is represented as only

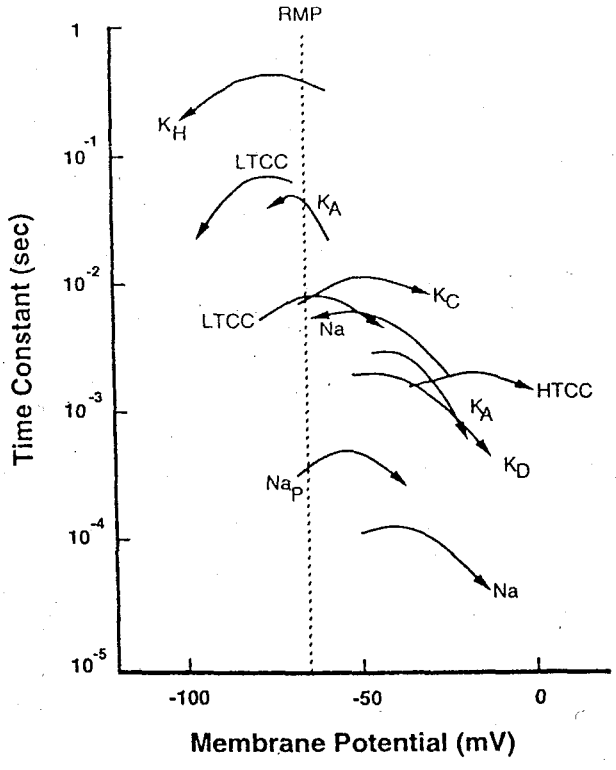

Fig 5. Time constants for different conductances over the voltage range of change in activation or inactivation. Activation curves (increase in conductance with depolarization) are indicated by rightward pointing arrows; inactivation curves (decrease in conductance with depolarization), by leftward arrows. Resting membrane potential (RMP) *is shown by the vertical dotted line. Na = fast sodium current; NaP = persistent sodium current; LTCC = low-threshold calcium current; HTCC = high-threshold calcium current; K_D = delayed rectifier; K_A = A current; K_H = H current (conducts both K^+ and Na^+); K_C = C current (at 500 nM intracellular Ca^{2+}).*

having an "inactivation curve" in Figure 5 since it activates with hyperpolarization (anomalous rectification). I_H had a time constant of 200 to 500 msec, much longer than that of LTCC, which had an activation time constant of 1 to 2 msec (see Fig 5). Therefore, during the brief period of LTCC activation leading to LTCS, I_H changed only infinitesimally and produced little effect. In order to explore other channel alterations that might alter the LTCS, we considered plausible alterations to channel kinetics suggested by known pharmacology or channel variability.

We first studied the effect of reducing the I_H time constant tenfold, to match the I_H time constant of 40 msec measured in cat sensorimotor cortex [29]. This change caused a reduction in the number of fast spikes in the LTCS, primarily due to a reduced hyperpolarization. When the current was increased to obtain the same hyperpolarization as before, the magnitude of the LTCS was restored. We then tried shifting the activation curve for I_H, a further manipulation suggested by the effect of beta-adrenergic compounds on I_H [30]. A 20-mV depolarizing shift in activation caused I_H to more directly oppose the activation of LTCC. On the other hand, the altered I_H produced less opposition to the initial hyperpolarization. The combination of time constant reduction and activation shift produced a reduction in LTCS in all parameter sets tested and entirely eliminated the LTCS in some parameter sets.

Voltage Shift of Low-Threshold Calcium Current Activation Can Produce Low-Frequency, Low-Threshold Calcium Spikes

The thalamic cell simulated above showed an intrinsic rhythmicity with a frequency of 10 Hz when activated by a hyperpolarizing pulse from its resting potential. The oscillation, which can be seen in any Hodgkin-Huxley–like system with suitable parameters, is an alternation of inward current–mediated depolarization turning on outward currents, which mediate hyperpolarization and turn on the next cycle of inward current. It was not possible to obtain slower repetitive bursting at the resting potential without altering the channel kinetics. Slow repetitive oscillations at rest could be obtained by increasing the time constant for LTCC inactivation fivefold to prolong the LTCS and the interburst interval. A 5-mV hyperpolarizing shift in the LTCC activation curve augmented the bursting. Figure 6 shows sustained 3-Hz spontaneous activity following an initial hyperpolarization. With these parameters, the 10-mV shift of LTCC activation seen with ethosuximide caused retention of the initial LTCS but loss of sustained repetitive bursting.

Alternatively, it was possible to obtain 3-Hz sustained oscillation by hyperpolarizing the model neuron with a sustained current injection in order to bring it into the range of LTCC/I_H interaction [31]. This corresponds to the slow-frequency oscillations observed with hyperpolarization in vivo that appear to be related to the delta rhythm of slow-wave sleep [32].

Discussion

Our modeling of the voltage-clamp data from Coulter and colleagues [3] has led to an unexpected conclusion regarding the underlying cause of ethosuximide's effect on the LTCC. They suggested that ethosuximide primarily altered either the number of channels available or the unitary conductance of the single channel without an effect on activation, inactivation, or channel time constants. Our best fit of their voltage-clamp data was obtained by shifting the activation curve to more depolarized potentials with only a small reduction in total LTCC permeability. By requiring that we explicitly define all elements of the voltage-clamp dynamics, the process of modeling helped to make this conclusion clear.

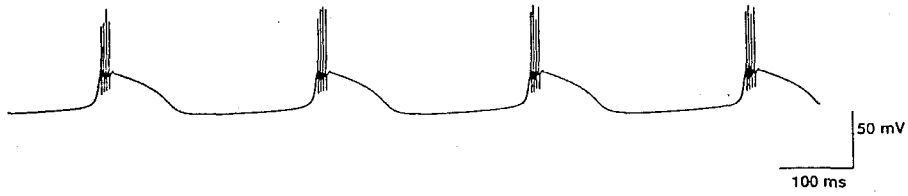

Fig 6. Three-hertz repetitive firing obtained by shifting the activation curve for the low-threshold calcium current to a more hyperpolarized location and slowing its kinetics fivefold. Bursting was initiated by releasing the cell from the hyperpolarizing current clamp and was self-sustained.

Our model supports the hypothesis of Prince's group that ethosuximide's reduction of LTCC amplitude seen in voltage clamp would eliminate the LTCS seen in current clamp. The traces that we simulated were obtained from tissue slice preparation. The cells in this study differ both in connectivity and in the nature of their input from physiological conditions. However, the primary behaviors elicited with current injection have also been seen in vivo [33]. Therefore, we anticipate that the alterations in behavior suggested by the computer model would also be pertinent to the cell's normal physiology. The reduction in the ability of the cell to participate in LTCSs in the presence of ethosuximide would be reflected in a reduced tendency to participate in network rhythms, such as absence epilepsy, that depend on this cellular response. The maintenance of the model cell's tonic response to depolarization in the presence of ethosuximide suggests that the cell's participation in other firing modes, particularly the relay mode critical to sensory perception, would be unaffected.

We used three studies of the LTCC in the thalamus to constrain our voltage-clamp data. These studies showed similar results across species, techniques, and thalamic areas. Despite this, the activation curve for the LTCC had to be varied significantly to reproduce specific voltage-clamp recordings taken from individual cells. The greater variability of this parameter might reflect a natural variability of the activation curve due to endogenous modulation by intracellular second messenger effects or extracellular paracrine influences [34]. Similar shifts in steady-state activation have been reported in several channels [30, 35]. If ethosuximide acts by shifting the activation curve as we suggest, this action might occur through alteration of an endogenous intrinsic modulator. Interestingly, LTCC has been shown to be sensitive to G-proteins in rat dorsal root ganglion neurons [36] and rat pituitary cells [37]. Although the mechanism of the LTCC alteration is not clear, the evidence is consistent with a depolarizing shift in activation in the presence of guanosine 5'-*O*(3-thio) triphosphate (e.g., see Fig 7C of [36]). Hence, G-protein activation might play a role in ethosuximide's effect.

The map of channel dynamics shown in Figure 5 can help determine which conductances are likely to be involved in a particular spiking pattern and suggest how alterations in conductances could interfere with this pattern. Computer modeling can further be used to suggest pharmacological manipulations to produce designer drugs that will have particular effects. As we have shown, I_H can either hinder or augment the LTCS depending on the voltage range. At resting potential, it opposed the genesis of the LTCS. At hyperpolarized potentials, however, I_H augments the LTCS by assisting in the depolarization toward LTCC threshold [31]. We predict that a drug designed to make I_H faster and shift its activation in the depolarizing direction would reduce LTCS.

It was possible to obtain slow bursting at the resting potential by combining an increase in the time constant of inactivation with a hyperpolarizing shift of the LTCC activation curve or by hyperpolarizing the model neuron. Both conditions put the bursting frequency in the 2- 3-Hz range observed in absence epilepsy. This suggests two different etiological processes that might predispose to absence epilepsy: a direct disorder of the intrinsic channels or a disorder of neuromodulators leading to hyperpolarization. Although it was possible to produce slow rhythms in the isolated cell model, we suspect that the properties of the network may be of great importance in establishing these rhythms in vivo. Preliminary simulations have shown that repetitive cortical synaptic input could alter the frequency of these slow oscillations over a wide range around the intrinsic resonant frequency of the neuron. Ethosuximide, by affecting the intrinsic rhythmicity, could also alter these entrainment patterns.

Our results support the hypothesis of Coulter and colleagues that ethosuximide's effect on the LTCC might eliminate LTCSs without affecting the response of the cell to other inputs. Future simulations will attempt to take the hypothesis one step further by modeling multiple thalamic cells with synaptic interactions between them. In this study, we used computer modeling both to extend our understanding of the pharmacological effect of ethosuximide on the cell and to predict other channel alterations that might produce similar effects. Accurate models of neurons and networks of

neurons could be of general use in predicting channel alterations that would prevent the pathological firing patterns of epileptic syndromes, helping to guide the use of in vitro channel assays to search for effective pharmacological agents.

Dr Lytton was supported by a Physician Scientist Award (K11 AG00382) from the National Institute of Aging. Dr Sejnowski is an investigator with the Howard Hughes Medical Institutes and was supported in part by the National Institute of Mental Health (MH46482-01A1).

We wish to thank C-F. Hsiao, M. Dubin, and J. Capowski for providing the thalamic cell tracing that formed the basis of our model and P. Bush, J. Wathey, and J. Jester for helpful discussions. A. Bell and P. S. Churchland suggested the format of the channel plot in Figure 5.

References

1. Aicardi J. Epilepsy in children. New York: Raven, 1986
2. Browne TR, Dreifuss FE, Dyken PR, et al. Ethosuximide in the treatment of absence (petit mal) seizures. Neurology 1975; 25:515–524
3. Coulter DA, Huguenard JR, Prince DA. Characterization of ethosuximide reduction of low-threshold calcium current in thalamic neurons. Ann Neurol 1989;25:582–593
4. Coulter DA, Huguenard JR, Prince DA. Specific petit mal anticonvulsants reduce calcium currents in thalamic neurons. Neurosci Lett 1989;98:74–78
5. Coulter DA, Huguenard JR, Prince DA. Differential effects of petit mal anticonvulsants and convulsants on thalamic neurones: calcium current reduction. Br J Pharmacol 1990;100:800–806
6. Williams D. A study of thalamic and cortical rhythms in petit mal. Brain 1953;76:50–69
7. Avoli M, Gloor P, Kostopoulos G, Gotman J. An analysis of penicillin-induced generalized spike and wave discharges using simultaneous recordings of cortical and thalamic single neurons. J Neurophysiol 1983;50:819–837
8. Pelligrini A, Dossi RC, Dal Pos F, et al. Ethosuximide alters intrathalamic and thalamocortical synchronizing mechanisms: a possible explanation of its antiabsence effect. Brain Res 1989; 497:344–360
9. Jahnsen H, Llinás R. Ionic basis for the electroresponsiveness and oscillatory properties of guinea-pig thalamic neurons in vitro. J Physiol (Lond) 1984;349:227–247
10. Suzuki S, Rogawski MA. T-type calcium channels mediate the transition between tonic and phasic firing in thalamic neurons. Proc Natl Acad Sci 1989;86:7228–7232
11. Hines ML. A program for simulation of nerve equations with branching geometries. Int J Biomed Comp 1989;24:55–68
12. Jones EG. The thalamus. New York: Plenum, 1985
13. Steriade M, Llinás RR. The functional states of the thalamus and the associated neuronal interplay. Physiol Rev 1988; 68:649–742
14. Hodgkin AL, Huxley AF. A quantitative description of membrane current to its application to conduction and excitation in nerve. J Neurophysiol 1952;117:500–544
15. Traub R. Simulation of intrinsic bursting in CA3 hippocampal neurons. Neuroscience 1982;7:1233–1242
16. Lytton WW, Sejnowski TJ. Inhibitory interneurons may help synchronize oscillations in cortical pyramidal neurons. J Neurophysiol 1991;66:1059–1079
17. Hille B. Ionic channels of excitable membranes. 2nd ed. Sunderland, MA: Sinauer Associates, 1992
18. Crunelli V, Kelly JS, Leresche N, Pirchio M. The ventral and dorsal lateral geniculate nucleus of the rat: intracellular recordings in vitro. J Physiol (Lond) 1987;384:587–601
19. Crunelli V, Leresche N, Parnavelas JG. Membrane properties of morphologically identified x and y cells in the lateral geniculate nucleus of the cat in vitro. J Physiol (Lond) 1987;390:243–256
20. Coulter DA, Huguenard JR, Prince DA. Calcium currents in rat thalamocortical relay neurones: kinetic properties of the transient low-threshold current. J Physiol (Lond) 1989;414: 587–604
21. Crunelli V, Lightowler S, Pollard CE. A T-type Ca^{2+} current underlies low-threshold Ca^{2+} potentials in cells of the cat and rat lateral geniculate nucleus. J Physiol (London) 1989;413: 543–561
22. Hernandez-Cruz A, Pape HC. Identification of two calcium currents in acutely dissociated neurons from the rat lateral geniculate nucleus. J Neurophysiol 1989;61:1270–1283
23. Bush PC, Sejnowski TJ. Simulations of a reconstructed cerebellar Purkinje cell based on simplified channel kinetics. Neural Comput 1991;3:321–332
24. McCormick DA, Pape HC. Properties of a hyperpolarization-activated cation current and its role in rhythmic oscillation in thalamic relay neurones. J Physiol (Lond) 1990;431:291–318
25. Fox AP, Nowycky MC, Tsien RW. Kinetic and pharmacological properties distinguishing three types of calcium currents in chick sensory neurones. J Physiol (Lond) 1987;394:149–172
26. Kay AR, Wong RKS. Calcium current activation kinetics in isolated pyramidal neurones of the CA1 region of the mature guinea-pig hippocampus. J Physiol (Lond) 1987;392:603–616
27. Wang XJ, Rinzel J, Rogawski MA. A model of the T-type calcium current and the low-threshold spike in thalamic neurons. J Neurophysiol 1991;66:839–850
28. Jahnsen H, Llinás R. Electrophysiological properties of guinea pig thalamic neurones: an in vitro study. J Physiol (Lond) 1984;349:205–226
29. Schwindt PC, Spain WJ, Crill WE. Influence of anomalous rectifier activation on afterhyperpolarizations of neurons from cat sensorimotor cortex in vitro. J Neurophysiol 1988;59:468–481
30. McCormick DA, Pape HC. Noradrenergic and serotonergic modulation of a hyperpolarization-activated cation current in thalamic relay neurones. J Physiol (Lond) 1990;431:319–342
31. McCormick DA, Huguenard JR, Strowbridge BW. Determination of state dependent processing in thalamus by single neuron properties and neuromodulators. In: McKenna T, Davis J, Zornetzer SF, eds. Single neuron computation. New York: Academic, 1991
32. Steriade M, Curró Dossi R, Nuñez A. Network modulation of a slow intrinsic oscillation of cat thalamocortical neurons implicated in sleep delta waves: cortically induced synchronization and brainstem cholinergic suppression. J Neurosci 1991; 11:3200–3217
33. Steriade M, Jones EG, Llinás RR. Thalamic oscillations and signaling. New York: Wiley, 1990
34. Llinás R, Geijo-Barrientos E. In vitro studies of mammalian thalamic and reticularis thalami neurons. In: Bentivoglio M, Spreafico R, eds. Cellular thalamic mechanisms. New York: Elsevier, 1988:23–33
35. Dascal N. Lotan I. Activation of protein kinase C alters voltage-dependence of a Na^+ channel. Neuron 1991;6:165–175
36. Scott RH, Wootton JF, Dolphin AC. Modulation of neuronal T-type calcium channel currents by photoactivation of intracellular guanosine 5′-*O*(3-thio) triphosphate. Neuroscience 1990; 38:285–294
37. Williams PJ, MacVicar BA, Pittman QJ. Synaptic modulation by dopamine of calcium currents in rat pars intermedia. J Neurosci 1990;10:757–763